Cassini Plasma Spectrometer and hybrid model study on Titan's interaction: Effect of oxygen ions

I. Sillanpää,[1] D. T. Young,[1] F. Crary,[1] M. Thomsen,[2] D. Reisenfeld,[3] J.-E. Wahlund,[4] C. Bertucci,[5] E. Kallio,[6] R. Jarvinen,[6] and P. Janhunen[6]

Received 5 January 2011; revised 13 April 2011; accepted 20 April 2011; published 23 July 2011.

[1] During the Cassini Titan flyby on 2 July 2006 (T15), Titan was surrounded by a magnetospheric plasma flow with density about 0.1 cm^{-3} as measured by Cassini Plasma Spectrometer (CAPS). A very low fraction of water group ions (O^+) was detected in the flow dominated by hydrogen ions. We show that Titan's plasma interaction can be highly sensitive to the small fraction of oxygen ions in the magnetospheric flow. The ion quantities of the magnetospheric flow during the flyby were obtained from numerical moments calculated from the CAPS measurements; the average ambient magnetic field was determined using the Cassini magnetometer data. We simulated the flyby using a global hybrid model; the water group abundance in the flow was varied in three simulation runs. Based on the simulation results, the oxygen content has an especially notable effect on the extent of Titan's induced magnetosphere. A multi-instrument analysis was performed comparing with the simulations, whereby a comprehensive picture of the plasma properties around Titan during this flyby was obtained. Comparisons between the hybrid model simulations and Cassini measurements during the flyby point toward O^+ density in the undisturbed magnetospheric flow having been around 0.008 cm^{-3}, which would have accounted for one half of the dynamic pressure of the flow.

Citation: Sillanpää, I., D. T. Young, F. Crary, M. Thomsen, D. Reisenfeld, J.-E. Wahlund, C. Bertucci, E. Kallio, R. Jarvinen, and P. Janhunen (2011), Cassini Plasma Spectrometer and hybrid model study on Titan's interaction: Effect of oxygen ions, *J. Geophys. Res.*, *116*, A07223, doi:10.1029/2011JA016443.

1. Introduction

[2] Titan provides a unique object for studying atmospheric interactions with a magnetized plasma flow. Among the largest natural satellites in the solar system (Titan's radius R_T = 2575 km), it is the only known satellite that has a dense atmosphere, a fully developed ionosphere, and an extensive exosphere. Titan orbits Saturn in the outer magnetosphere of Saturn at a radial distance between 19.69 R_S and 20.86 R_S from Saturn (Saturn's equatorial radius R_S = 60268 km). Occasionally Titan can enter the magnetosheath in the noon sector [*Bertucci et al.*, 2008]. Titan's interaction with the surrounding Saturnian plasma and magnetic fields has been a focus of intense study, both analytical and numerical, since the Voyager 1 spacecraft passed through Titan's plasma wake on 12 November 1980.

[3] This interaction is characterized by several key features. 1) Titan has a magnetosphere induced by the ambient plasma flow and by the interaction with the magnetic field of Saturn (no internal magnetic field has been observed [*Neubauer et al.*, 2006]). 2) The escape of gas from Titan's atmosphere and ion pickup processes have major effects on the vicinity of Titan through mass loading and ionization of the exosphere [e.g., *Hartle et al.*, 2006]. 3) Saturn's magnetosphere is dynamic and its magnetopause responds to changes in the solar wind pressure. 4) The current sheet of Saturn's magnetosphere is constantly shifting, especially on the night side [*Simon et al.*, 2010]. Therefore Titan encounters a highly variable plasma stream that is constantly modified by the many different external and internal forces acting on Saturn's magnetosphere. 5) The ambient plasma flow is partly deflected by the magnetic buildup around Titan's ionosphere and partly impinging on its upper atmosphere [e.g., *Sillanpää et al.*, 2007].

[4] The Cassini mission to Saturn has made the study of Saturn's system one of the most exciting and discovery-rich endeavors in space and planetary sciences. The main phase of the mission began with the insertion of the Cassini spacecraft into an orbit around Saturn in June 2004.

[5] So far the mission has accomplished about 70 close flybys of Titan. Such a large number of flybys and the associated in situ measurements have enabled valuable new

[1]Space Science and Engineering Division, Southwest Research Institute, San Antonio, Texas, USA.
[2]Los Alamos National Laboratory, Los Alamos, New Mexico, USA.
[3]Department of Physics and Astronomy, University of Montana, Missoula, Montana, USA.
[4]Swedish Institute of Space Physics, Uppsala, Sweden.
[5]Institute for Astronomy and Space Physics, Buenos Aires, Argentina.
[6]Finnish Meteorological Institute, Helsinki, Finland.

0148-0227/11/2011JA016443

statistical studies. *Rymer et al.* [2009] divided Cassini flybys of Titan into several categories based on the characteristics of the electron spectra during 3 h before and after the closest approach. Other recent work [*Bertucci et al.*, 2009; *Simon et al.*, 2010] has focused on the magnetic environment at Titan's orbit and during the flybys. These studies have shown that the outer reaches of Saturn's magnetosphere are buffeted by the varying solar wind causing it to contract and expand accordingly and giving rise to significant variability in the plasma and magnetic characteristics around Titan's orbit; this is true even when Saturn's magnetopause is not very close to the orbit. Moreover, Bertucci et al. [see also *Arridge et al.*, 2008] concluded that aside from Saturn's seasonal and solar wind pressure effects, the plasma content and magnetic field near Titan's orbit correlates strongly with Saturn's kilometric radiation emissions.

[6] The magnetospheric variability is also demonstrated in a recent study of moments of the plasma distribution function (density, velocity, temperature, and pressure) by *Thomsen et al.* [2010]. The plasma moments were calculated from the ion measurements by the Cassini Plasma Spectrometer (CAPS) throughout Saturn's magnetosphere. (Thomsen et al.'s method is described in section 3.) Those results show that the variability of plasma density (consisting primarily of H^+, H_2^+ and water group ions) increases with radial distance from Saturn, especially beyond $r > 15\ R_S$.

[7] In a recent study of Cassini encounters T9 and T18, *Sittler et al.* [2010] used CAPS and Cassini magnetometer measurements to provide plasma quantities for a very low density plasma interaction at Titan. During these flybys Titan was on the south side of Saturn's current sheet in the predawn sector where the ambient plasma flow around Titan was composed predominantly of light H^+ and H_2^+ ions. The electron and ion densities of the flow were measured at about 3×10^{-3} cm^{-3}.

[8] Several statistical studies on Titan's upper atmosphere and ionosphere by combining numerous flyby measurements have also been published in recent years. *Ågren et al.* [2009] studied the ionospheric density and temperature profiles using the voltage sweep data from the Langmuir probe on board the Cassini spacecraft. *Edberg et al.* [2010] used the same data now extended to 52 flybys and showed that there is a logarithmic dependence between the ionospheric densities and temperatures. Latest in a series of upper atmosphere composition studies using the Cassini Ion and Neutral Mass Spectrometer results is a study by *Magee et al.* [2009].

[9] Simulations of the plasma interaction at Titan have proven to be necessary in order to obtain an accurate picture of the complex processes at work there. Global models (i.e., fully three-dimensional models covering most of the interaction region around Titan) in particular have made a remarkable contribution. However, many of the characteristics of the upstream plasma flow used in most simulations are a priori values.

[10] The first three-dimensional magnetohydrodynamics (MHD) models, which use a single-fluid description for all particle species, showed the magnetic draping pattern around Titan [*Kabin et al.*, 1999; *Kopp and Ip*, 2001; *Nagy et al.*, 2001]. Test particle modeling has been used to study ion fluxes flowing into Titan's exobase [*Ledvina et al.*, 2005; *Tseng et al.*, 2008]. These studies use fields from ideal MHD models to calculate the ion trajectories.

[11] More recently, a multispecies Hall-MHD model [e.g., *Ma et al.*, 2006] has been implemented to model Titan's plasma interaction. This model uses a collapsed chemical scheme with seven proxy species to represent the ions and their reactions. In the model the simulation grid is logarithmically spaced and spherical. Furthermore, multifluid MHD simulations [*Snowden et al.*, 2007; *Winglee et al.*, 2009] have been utilized to study Titan's plasma environment. The multifluid MHD approach takes into account the movement of different ion species whereas in the single-fluid MHD all ions have the same local velocity.

[12] In the hybrid approach the ion kinetics are calculated self-consistently and with unconstrained velocity distributions, while electrons form a charge-neutralizing fluid. The electron fluid is often considered noninertial (i.e., massless) in hybrid models; even then the electron pressure forcing can be included if the electron temperature is defined. Hybrid modeling has shown the asymmetric wake structure caused by the finite gyroradius of the pickup ions originating at Titan and the ions of the incident flow [e.g., *Kallio et al.*, 2004, 2007; *Simon et al.*, 2006; *Simon and Motschmann*, 2009].

[13] Recent results from global simulations have been able to reproduce important characteristics of Titan's plasma interaction such as the key features of the magnetic field in the wake, and in some cases the electron density comparisons have also been made [*Ma et al.*, 2006; *Modolo et al.*, 2007]. However, more detailed comparisons with ion measurements are in order, and that is one of the motivations for the present study.

[14] The main goals of this paper include describing the effects that changes in the plasma composition can cause in the Titan's plasma and magnetic wake when the total ion density of the magnetospheric flow is roughly known. Furthermore, by comparing simulation results with data from several of Cassini's plasma instruments, we show that the probable oxygen ion density of the upstream plasma flow can be determined. Several key features of Titan's plasma interaction are also reviewed from simulation and data points of view.

[15] Our study is limited to a case study, namely to Titan wake flyby T15, that was marked by a upstream magnetospheric flow that was predominantly hydrogen (both atomic and molecular). The flyby geometry is described in section 2. In section 3 we present briefly the method for obtaining ion moments from the CAPS instrument. These moments were used to estimate the undisturbed flow conditions during the flyby. Sections 4 and 5 give an overview of the HYB-Titan model and the parameters used in the simulation runs for this study.

[16] Then the measurements by Cassini instrumentation for the flyby are presented and compared with the simulation results in section 6. The results are discussed in a larger context in section 7 and finally summarized.

[17] In this work we use the Titan-centered TIIS coordinates, where the X axis points in the direction of Titan's orbital motion, the Y axis points from Titan to Saturn, and the Z axis completes the right-handed coordinate system and is perpendicular to Titan's orbital plane (close to northward).

2. Titan Flyby T15

[18] The 15th close flyby of Titan (T15) by the Cassini spacecraft took place on 2 July 2006 (day of year 183). The

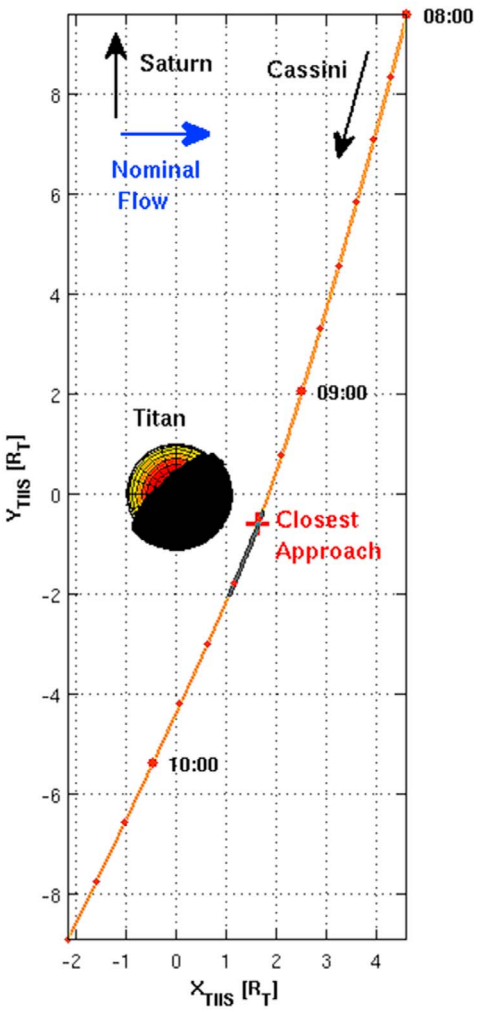

Figure 1. The trajectory of the Cassini Titan flyby T15 was very close to Titan's orbital plane. The view is from north of the orbital plane. The dark portion of Titan shows the part in shadow during the flyby; also the portion of the trajectory that was in the shadow of Titan's solid body, is indicated.

spacecraft was on an outbound leg of an elliptical orbit around Saturn while it passed through Titan's wake. Figure 1 illustrates the trajectory with respect to Titan's solid body. The part of the trajectory shown covers the time period from 8:00 to 10:30 UTC. During this period the speed of the spacecraft decreased from 6.8 to 6.0 km/s with respect to Saturn; with respect to Titan the speed was about 5.6 km/s before and after the encounter.

[19] The closest approach at 09:21 UTC was at an altitude of 1905 km ($r = 1.74\ R_T$). In Titan's vicinity the trajectory was very close to the orbital plane of Titan ($|Z_{TIIS}| < 0.01\ R_T$). During the flyby Titan was between dusk and midnight in Saturn's magnetosphere with Saturn local time (SLT) 21.20 h. The subsolar latitude was 16.8° south. The spacecraft was in the nominal wake of Titan from 09:08 to 09:24 UTC and in the shadow of Titan's solid body from 09:19 to 09:32 UTC. A nominal situation refers to a geometry in which the direction of magnetospheric flow is aligned with Titan's orbital motion.

3. CAPS Moments

[20] Ion moments for several quantities of the local plasma flow can be obtained from CAPS data. One of the methods is a numerical integration of electrostatic analyzer data from the ion mass spectrometer (IMS) that is part of the CAPS instrumentation [see also *Thomsen et al.*, 2010; *Thomsen and Delapp*, 2005]. This method for the so-called INUM moments is briefly summarized as follows. The IMS instrument consists of a top hat electrostatic analyzer with eight anode detectors and a time-of-flight analyzer [*Young et al.*, 2004]. The electrostatic analyzer gives energy per charge (E/q) values for incident ions. It is followed by a time-of-flight analyzer, which essentially gives mass per charge counts with a much lower detection efficiency than the electrostatic analyzer. The time-of-flight analyzer has two sensors: a high-resolution sensor facilitated by varying electric field and a "straight-through" sensor, that has better detection efficiency. CAPS has an actuator that allows a coverage of about 2π sr for the instrument. While the electrostatic analyzer yields actuator and detector information (i.e., direction), the time-of-flight data are usually analyzed in data sets summed over one or more sweep cycles and over all eight detectors.

[21] The process of calculating the INUM plasma moments begins with the counts of the electrostatic analyzer being partitioned into three ion groups: H^+, H_2^+/He^{++}, and water group ions W^+ which include ion species O^+, OH^+, H_2O^+, and H_3O^+. The partitioning is accomplished by fitting a time-of-flight spectrum from the straight-through analyzer to model peaks at each energy level.

[22] The plasma moments are derived iteratively by filling in the undetected directions (e.g., by mirroring) and calculating resulting moments for each ion group i from the velocity distribution functions $f_i(\vec{v})$. Thus, it is essential that the peak of the ion distribution be within the field of view of the instrument. The INUM moments for density, flow velocity and the temperature tensor are defined as follows:

$$n_i = \int_{all\ \vec{v}} f_i(\vec{v}) \mathrm{d}^3\vec{v} \tag{1a}$$

$$\vec{V}_i = \frac{1}{n_i} \int_{all\ \vec{v}} \vec{v} f_i(\vec{v}) \mathrm{d}^3\vec{v} \tag{1b}$$

$$\mathbf{T}_i = \frac{m_i}{n_i} \int_{all\ \vec{v}} \left(\vec{v} - \vec{V}_i\right)\left(\vec{v} - \vec{V}_i\right) f_i(\vec{v}) \mathrm{d}^3\vec{v} \tag{1c}$$

Thomsen et al. [2010] performed comparisons especially of the total ion densities derived from the INUM moments with Cassini measurements of electron density by the Radio and Plasma Wave Science instrumentation and the Langmuir probe. They found the agreement in general to be better than a factor of 2.

4. Description of HYB Hybrid Model for Titan

[23] In the hybrid approach to plasma simulations, ion kinetics are modeled self-consistently with the dynamical electromagnetic fields. Thus hybrid models are especially

well suited for the study of the plasma interaction at Titan, where ion gyroradii are of the order of Titan radius for both the ions of the incident flow and the pickup ions.

[24] The HYB simulation model is a particle-in-cell code developed at the Finnish Meteorological Institute around 2007 when several global hybrid simulation models were parameterized and combined in a single code framework [see *Sillanpää*, 2008]. The HYB model for Titan (HYB-Titan) used in this study is based on an updated version of this general code.

[25] This simulation code uses a hierarchical grid structure to store and propagate the field quantities. The cubical cells of the Cartesian base grid can be divided each to eight new grid cells that are half the size of the base cell. The process dividing the grid cells can be further iterated. This makes it easy to control the resolution of the grid; in this study we have used cell sizes of 0.2 and 0.4 R_T in most of the simulation domain. Resolution of 0.1 R_T was used within 2 R_T from Titan on the ramside and 3 R_T into the wake, while right at the outer boundaries the cells were undivided and had the size of the base cells 0.8 R_T. The rectangular simulation domain was aligned with the flow direction and extended 12.8 R_T into the wake of Titan, 6.4 R_T in the ram direction and 12 R_T to the four sides perpendicular to the undisturbed flow.

[26] Specifically there are six faces (each shared with one neighboring cell), eight nodes (each shared with seven neighboring cells), and one cell "center" associated with each cube-shaped grid cell; these are the actual location entities for the discretized fields. These cells form a staggered grid reminiscent of Yee-lattice and allow propagation of the discretized magnetic field without introducing any divergence larger than rounding errors; thus the magnetic field remains consistent with Gauss's law for magnetism ($\nabla \cdot \vec{B} = 0$).

[27] In the simulation ion species are represented with simulation particles. The simulation particles are actually cell-sized clouds, which represent a number of ions of a certain species (this number is called particle weight). The motion of a simulation particle is determined as the motion of a single particle of the same species located at the center of the cloud. Accumulation is the process of calculating needed discretized field quantities from the simulation particles. That cell-by-cell process is accomplished by determining the intersecting volume of each simulation particle (or cloud) found within the cell boundaries. That intersection volume and the corresponding weight are taken into account when the cell values for ion velocity $\vec{U}_i$ and charge density ρ_q are calculated.

[28] A major efficiency benefit in the model comes not only by adjusting the grid size appropriately, but even more importantly by controlling the average number of simulation particles per cell. Typical target values for the HYB-Titan model are 60 or more simulation particles per cell. This is accomplished by splitting and coalescencing simulation particles while conserving energy, momentum and angular momentum of the affected simulation particles as well as the total number of ions represented by them. A splitting ("one to two") or coalescencing ("three to two") step was allowed only once per cell per time step in previous versions of the model. This has been adjusted so that two or three such events can take place if the current particles-per-cell number differs from the target value by a factor that is more than 2. This allows better control of the particle number around locations where the grid resolution changes.

[29] The equations of the hybrid approach give a closed set of equations for propagation of particle positions and velocities and the magnetic field from their initial values. The model equations are as follows:

$$n_e = \frac{1}{e}\sum_i q_i n_i \tag{2a}$$

$$\vec{j} = \sum_i q_i n_i \vec{U}_i - e\, n_e \vec{U}_e \tag{2b}$$

$$\vec{E} = -\vec{U}_e \times \vec{B} - \frac{\nabla p_e}{e\, n_e} + \frac{\vec{j}}{\sigma} \tag{2c}$$

$$\nabla \times \vec{B} = \mu_0 \vec{j}. \tag{2d}$$

$$\nabla \times \vec{E} = -\frac{\partial \vec{B}}{\partial t} \tag{2e}$$

$$\frac{\mathrm{d}\vec{v}_i}{\mathrm{d}t} = \frac{q_i}{m_i}\left(\vec{E} + \vec{v}_i \times \vec{B}\right) - \vec{r}\frac{GM_T}{|\vec{r}|^3} \tag{2f}$$

$$\frac{\mathrm{d}\vec{x}_i}{\mathrm{d}t} = \vec{v}_i \tag{2g}$$

Charge neutrality (equation (2a)) is a fundamental assumption in the hybrid modeling approach, and typically not a concern as the Debye length is of the order of 100 m in planetary magnetospheres and in Titan's ionosphere; the smallest cell size of HYB-Titan model is three decades larger (see above).

[30] The quantities needed to calculate the evolution of the simulation during a single time step are the initial positions and velocities of the simulation particles representing the ion species and the magnetic field. From these the particle data is accumulated to field quantities for each simulation cell, namely ion velocity $\vec{U}_i$ and ion charge density ρ_q. Electric field is calculated from the Ohm's law (equation (2c)), where electron velocity $\vec{U}_e$ is obtained from equation (2b). Electric current $\vec{j}$ used in equation (2b) is the curl of magnetic field (equation (2d)). Finally, the curl of the electric field yields the change of the magnetic field for one time step as given in Faraday's law of induction (equation (2e)). The new, updated magnetic field is that with which the propagation of the fields for the following time step is calculated.

[31] It is the Lorentz force (equation (2f)) that gives the acceleration for ion particles. Hence the simulation particles have appropriate gyromotion and are affected by any drift motions that the electromagnetic fields present would create in nature. Gravity is included as an additional force in this equation. The group of hybrid model equations becomes finally a closed set with inclusion of the spatial propagation for particles (equation (2g)); the new particle locations are calculated directly from the updated velocities of the particles.

[32] The numerics of the HYB model have been described in detail in a dissertation by *Sillanpää* [2008]. Recently the HYB model has been implemented with an option to do repeated interpolations of electric field $\vec{E}$ or the accumulated charge density ρ_q between cell nodes and cell center. This is done in order to accomplish a spatial smoothing of these quantities before calculating the time step change of the magnetic field ($\Delta\vec{B}$). For the Titan model, using both types of smoothing interpolations has resulted in much increased stability and has made it unnecessary to use resistivity at the outer edges of the simulation area or where the grid resolution changes. Hence no artificial resistivity is used in the simulations presented here (however, in general all numerical simulations include some resistivity due to the discretization and other numerics involved).

[33] As a further improvement, we use an electron density background based on measurements by Cassini's Langmuir probe for Titan's ionosphere [*Ågren et al.*, 2009]. This ionospheric density provides adequate inner boundary for the simulation (field quantities such as electron velocity $\vec{U}_e$ need no cutoff altitude to be specified). This also provides a consistent electron pressure around the ionosphere, that contributes to particle motion by exerting an upward forcing (a constant ionospheric electron temperature T_e is used to calculate the pressure).

5. Simulation Runs for the T15 Flyby

[34] The characteristics of the upstream plasma flow during the T15 flyby were needed for the simulation runs of this study. We relied on the numerical moments from the CAPS plasma spectrometer for the ion quantities of the magnetospheric flow; these INUM moments provide values to quantify the plasma flow outside the main interaction area around Titan. Further, Cassini magnetometer data provided the orientation and magnitude of the ambient magnetic field $\vec{B}$. The T15 flyby was classified by *Rymer et al.* [2009] a plasma sheet encounter with brief occurrences of bimodal plasma background. Their work used the observations of the CAPS electron spectrometer spanning 3 h before and after the closest approach. The magnetometer measurements, on the other hand, indicate that during the encounter Titan was in the southern magnetic lobe of Saturn's magnetosphere.

[35] The CAPS pointing during the flyby was such that the field of view of IMS instrument covered the corotation direction during the ingress of the T15 flyby. During the egress after 10:00 UTC the corotation direction was slightly off the field of view, although the pointing would have covered the ambient flow direction if the flow was indeed turned away from Saturn like the INUM moments indicate. However, in practice even with good pointing the moments calculations can often have caveats; for example, the background noise level can be high or the rotations of the spacecraft may interfere with the results. There are flags in the INUM moments products indicating the quality of the moments for each of the three ion groups: whether 15 iterations were enough to find a single convergent value ("iterations were successful") and whether the signal-to-noise ratio was above certain limits. In this data set the good signal flag required that the iterations were successful.

[36] Figure 2 shows all the INUM moments calculated for the time period 06:00 UTC to noon in spherical coordinates centered on Saturn. Two significant rotations of the Cassini spacecraft (at 08:22–08:35 and 09:53–10:18 UTC) are indicated in the plot; the moments calculated at those times are consequently less reliable. Also the time period when cold ionospheric ions where encountered is indicated (see Figure 8 and associated text in section 6.3). These cold ions cause the most prominent features seen in all the moments. Here we focus, however, on the characteristics of the ambient plasma.

[37] The calculated plasma moments exhibit high level of variability until 07:10 UTC. There is a probable unphysical cause for this: up to 08:20 UTC the IMS field of view covered mostly the northern hemisphere. The θ components of the ion velocities had near-zero values from 06:00 to 07:00 UTC, and this can be an indication that the peak of the ion flux may have been out of the field of view during this interval.

[38] The ion density is dominated by atomic hydrogen with density estimated at 0.07 cm^{-3}. Molecular hydrogen ions provides about a quarter of the total ion density. This fraction is slightly higher in the egress. The water group ions remain at or below 0.01 cm^{-3} during the ingress. The magnetic field measurements for the whole day (2 July 2006, not shown) confirm that the Cassini spacecraft was mostly in the southern lobe of Saturn's magnetic field (magnetic field was in average about [2, 4, −1.5] nT in TIIS coordinates). There are two times during the 06:00 UTC to noon period when the spacecraft entered the northern lobe of Saturn's magnetosphere indicated by reversal of X and Y components of the magnetic field. First one lasted no more than 30 min around 07:15 UTC coinciding with a drop in the ion densities at 07:10–07:30 UTC. The second episode was from about 11:40 to 12:30 UTC. This coincides with the change in the composition of the magnetospheric flow when the water group dominates the ion density beginning at 11:20 UTC (this second northern lobe period is not fully included in Figure 2).

[39] The dominant component of the flow velocity, ϕ (along the corotation direction) seems to diminish for H_2^+ and W^+ as the spacecraft approaches Titan. The same trend is seen in the thermal velocities of all the ion groups. The flow has a significant deflection from the corotation direction during this flyby: the radial component (away from Saturn) is about 20 to 50 km/s during the ingress and about 50 km/s during the egress after the second spacecraft turning. The θ component (southward along Saturn's rotation axis) ranges from −10 to 50 km/s during ingress (the near zero values before 08:20 UTC unreliable as explained earlier in this section). During egress the θ component varies from 20 to 50 km/s for H^+ and H_2^+ until falling below −30 km/s at 11:40 UTC. Moments for the water group ions are available only after 11:00 UTC in the egress and they indicate similar behavior.

[40] The magnetometer data from the flyby is shown in Figure 3. For now we focus on the ambient magnetic field, and the magnetic field in the interaction region is discussed in section 6.1. Before and after passing through the main Titan interaction region, the Cassini magnetometer detected very similar values for the X and Y components (in TIIS coordinates) of the magnetic field. In the Z component the average values during the ingress and the egress differed by little more than 1 nT. There was a quick twist of the

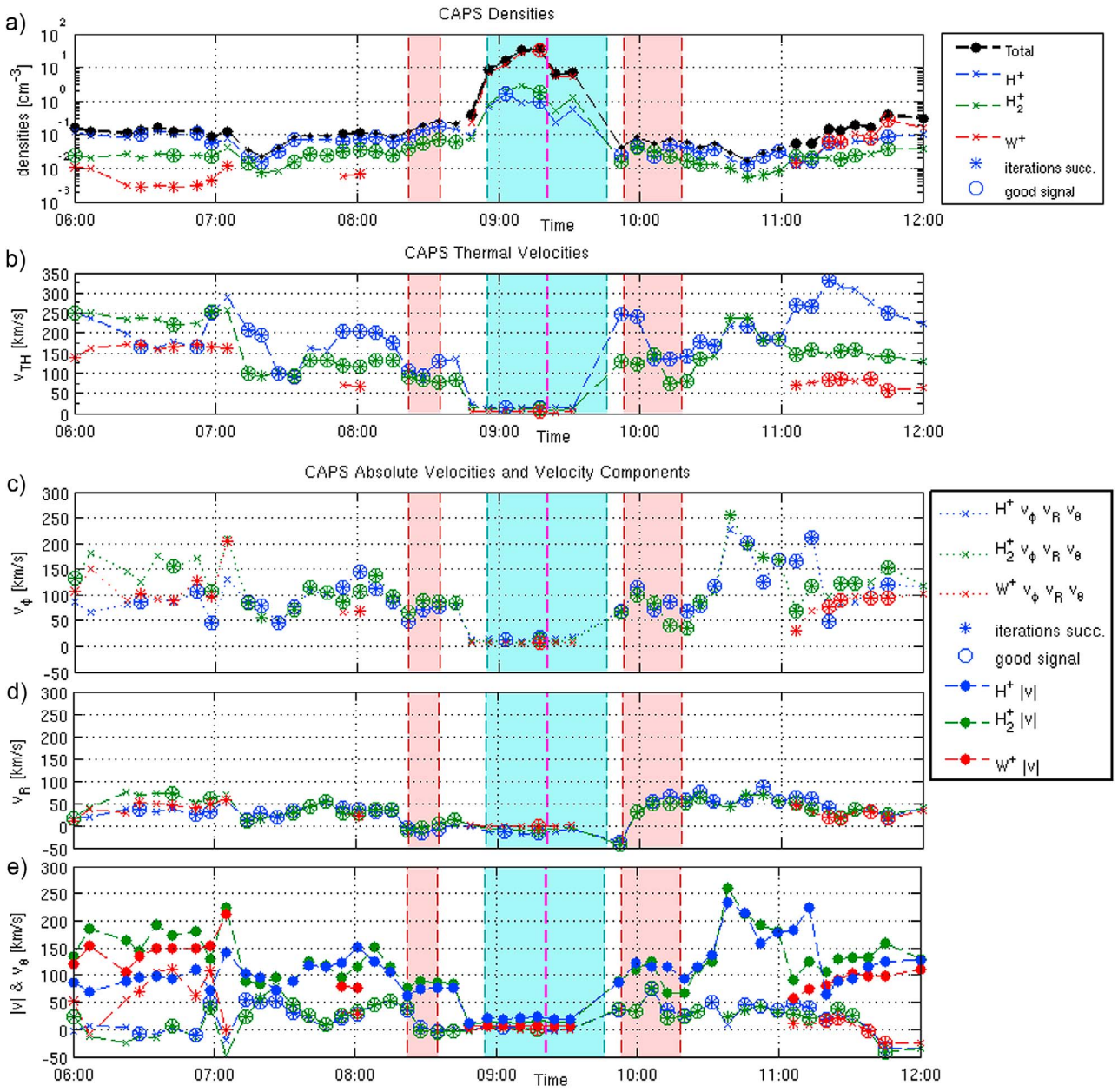

Figure 2. Ion moments (INUM) for density, thermal velocity and velocity components calculated from CAPS ion mass spectrometer measurements from 06:00 to 12:00 UTC with the closest approach of T15 at 09:21 UTC (magenta dashed line). (a) The ion densities, (b) the ion thermal velocities and (c–e) the velocity components: ϕ component (Figure 2c), the radial component (Figure 2d) and both the absolute velocities and the θ component (Figure 2e). For density values, thermal velocities, and the velocity components the quality of the moments is indicated (i.e., whether iterations were converged successfully or the signal-to-noise ration was high). The velocity components are given in Saturn-centered spherical coordinates (these spherical coordinates correspond to TIIS coordinates as follows $\phi \equiv X_{\mathrm{TIIS}}$, $r \equiv -Y_{\mathrm{TIIS}}$, $\theta \equiv -Z_{\mathrm{TIIS}}$, the discrepancy is less than 1%). The pale blue area indicates when an encounter with cold ionospheric plasma took place, and the pale red areas mark times when the spacecraft was rotated.

magnetic field at 10:00 UTC that is most clearly seen as a spike in the Z component that takes the Z component from below −3 nT to 0 nT and then below −4 nT. The absolute magnetic field is about 1 nT larger around this event that may extend from 09:52 to 10:05 UTC. The CAPS ion measurements for this period were affected by the turning of the spacecraft so they do not likely provide further insight. This period was not included in the upstream estimate taken as an average of periods 08:00–08:40 and 10:06–10:30 UTC.

[41] When making final estimates for the upstream conditions of the simulations, the values obtained from the INUM moments close to 08:00 UTC were given more emphasis (the spacecraft was then about 10 R_T away from Titan) and the values in the egress were not taken into

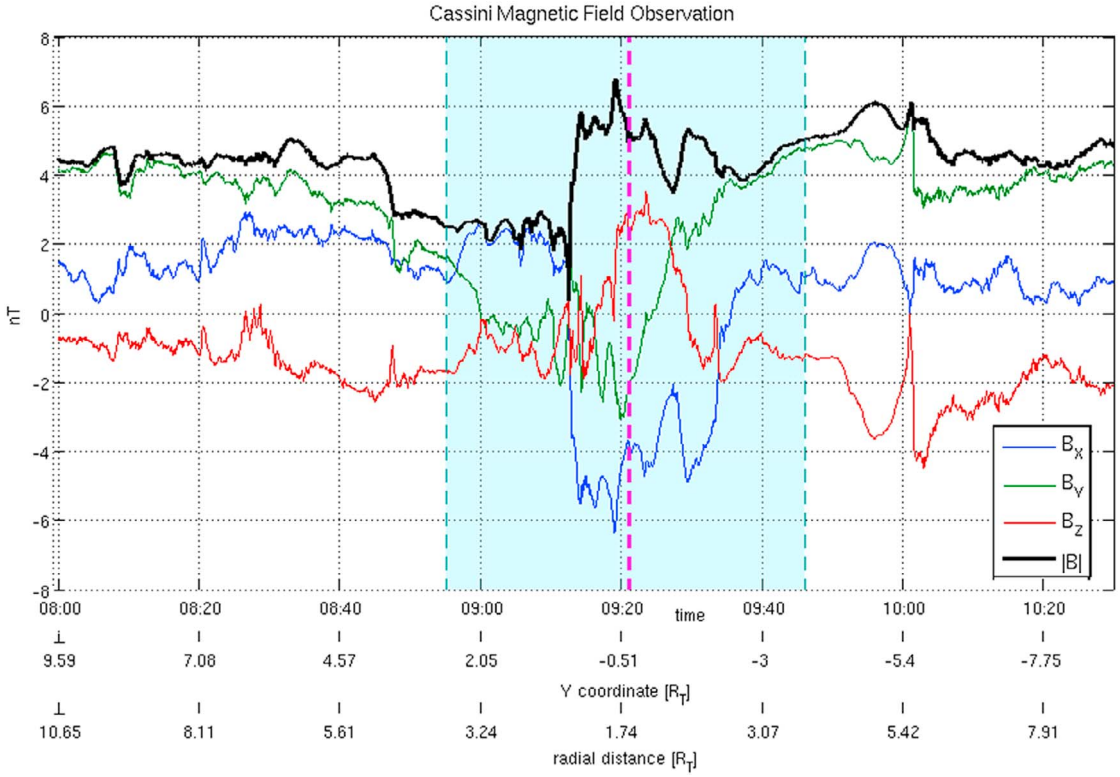

Figure 3. Cassini magnetometer data during the T15 flyby. The ionospheric ion region and the closest approach are indicated as in Figure 2.

account (the corotation direction was not in the field of view). We take the water group ions W^+ to be O^+ ions based on the identification of the heavier flow ions in an analysis by *Hartle et al.* [2006] for the first close Titan encounter (TA) by the Cassini spacecraft. The estimated plasma values for the undisturbed flow determined the three-species plasma flow inserted into the simulation domain in the simulation runs. Table 1 lists these quantities as well as some derived values.

[42] Based on CAPS electron spectrometer data of the ingress and egress of the T15 flyby, an electron temperature of 100 eV was taken into account for the sonic speed. The average magnetic field magnitude from the Cassini magnetometer data deviates a little from that calculated from the average component values. In the model the magnetic field components of the upstream magnetic field were used as the upstream values, and consequently the magnitude of the upstream field in the simulation was 4.35 nT (rather than the average magnetic field magnitude 4.47 nT). Interestingly, the estimated upstream flow direction and the average upstream magnetic field were nearly perpendicular.

[43] The estimate for the density of the water group (O^+) ions in the upstream flow was based on only a few successful moment calculations. Because of much larger mass of oxygen compared to hydrogen, oxygen ions even with the low density of 0.08 cm^{-3}, as per the estimate, contributed about a half of the dynamic pressure. To compensate for the uncertainty in the oxygen content in the flow, and consequently, also in the total dynamical pressure of the plasma flow, it was decided that the density of oxygen ions was to be varied between several simulation runs. For this purpose

Table 1. Estimated Plasma Values and Some Derived Values

Parameter	Value
INUM Moments	
H^+ density	0.07 cm^{-3}
H_2^+ density	0.03 cm^{-3}
O^+ density	0.008 cm^{-3}
H^+ thermal velocity	200 km/s
H_2^+ thermal velocity	120 km/s
O^+ thermal velocity	70 km/s
Bulk velocity	
$\vec{U}$ (X, Y, Z in TIIS)	[100, −30, −28] km/s
$\lvert\vec{U}\rvert$	108 km/s
Flow deviation from corotation	
Radially outward	16.7°
Southward	15.0°
Magnetic Field	
B_X	1.32 ± 0.69 nT
B_Y	3.88 ± 0.34 nT
B_Z	−1.46 ± 0.69 nT
$\lvert B\rvert$	4.47 ± 0.23 nT
Derived Quantities	
Mass density	0.259 amu/cm^3
Ion plasma pressure	22.4 eV/cm^3
Dynamic pressure	15.7 eV/cm^3
Sonic speed	144 km/s
Alfvén speed	187 km/s
Angle between $\vec{U}$ and $\vec{B}$	93°
$\vec{E}_C = -\vec{U} \times \vec{B}$	[−152 −109, −428] μV m
$\lvert\vec{E}_C\rvert$	467 μVm
Angle between $\vec{E}_C$ and $-Z_{\mathrm{TIIS}}$	23.7°

Table 2. O^+ Densities for the Upstream Flow in the Hybrid Simulation Runs and the Dynamic Pressures, Mass Densities, and Total Ion Densities for the Flow[a]

Run	n (O^+) (cm^{-3})	p_{dyn} (O^+ Fraction) (eV/cm^3)	ρ (O^+ fraction) (amu/cm^3)	n_i (O^+ Fraction) (cm^{-3})
1	0.003	10.8 (27%)	0.179 (27%)	0.103 (2.9%)
2	0.008	15.7 (49%)	0.259 (49%)	0.108 (7.4%)
3	0.014	21.5 (63%)	0.355 (63%)	0.114 (12%)

[a]The percentile contribution by oxygen ions is also given.

three simulations runs were made using the best estimate for oxygen density and two other values for one significantly lower and one higher density value for oxygen ions. The O^+ densities, the resulting dynamic pressures p_{dyn} as well as the total mass and ion densities (ρ and n_i, respectively) for these runs are given in Table 2. Otherwise the run parameters followed those given above.

[44] There was also a fourth simulation run made with no water group ions in the plasma flow to provide a control case where only hydrogen made up the incident plasma flow. For this run the magnetic field values were the same as in Table 1, and the plasma flow values were very similar to those listed above (another estimate based on the same INUM moments). The total ion density in the upstream flow for this run was 0.105 cm^{-3}. The corresponding mass density was 0.131 amu/cm^3 and the plasma and dynamic pressures were 17.9 and 8.48 eV/cm^3, respectively.

[45] In the simulations three pickup ion species were used: molecular nitrogen ions (N_2^+) were created uniformly at the exobase with small outward velocity. Methane and molecular hydrogen ions (CH_4^+ and H_2^+) where created based on photoionization rates and neutral density profiles from Cassini measurements [*Garnier et al.*, 2007] in the sunlit areas of Titan's exosphere.

6. Comparisons With Cassini Measurements

[46] Several instruments onboard the Cassini spacecraft provide measurements of plasma parameters, that can be used as a valuable check for the simulation results. Now we proceed to present the measurements of magnetic field, electron density, and ion energies and compare them with the simulations in order to understand the plasma interaction during the T15 flyby. We will also assess the validity the simulation results based on the Cassini plasma measurements.

6.1. Magnetic Field Along the Cassini Trajectory

[47] The magnetic field observations by the Cassini magnetometer for the T15 flyby are replotted in Figure 4a, and the magnetic fields along the Cassini trajectory in the three simulation cases are shown in Figures 4b–4d at the same scale. Several of the main features of the magnetometer measurements are found in the corresponding simulation results. These include the sharp drop in the B_X component from positive to negative values before the closest approach ($\Delta B_X \approx -8$ nT in the magnetometer data), the reduced magnitude of the magnetic field during the ingress (09:47–09:11 UTC in the magnetometer data), and increased absolute magnetic field in and around Titan's optical shadow (about 09:12–09:35 UTC in the magnetometer data).

[48] To properly interpret the results, the principles controlling the formation of the induced magnetosphere of Titan as well as the associated electric currents should be understood. As the magnetized plasma of Saturn's magnetosphere encounters Titan's exosphere and ionosphere, the flow is both diverted by the ionospheric currents and slowed down due to the mass loading by newly ionized exospheric particles and ionic matter escaping from the ionosphere. The magnetic disturbances in typical Titan conditions propagate with the Alfvén speed. Consequently the magnetic field

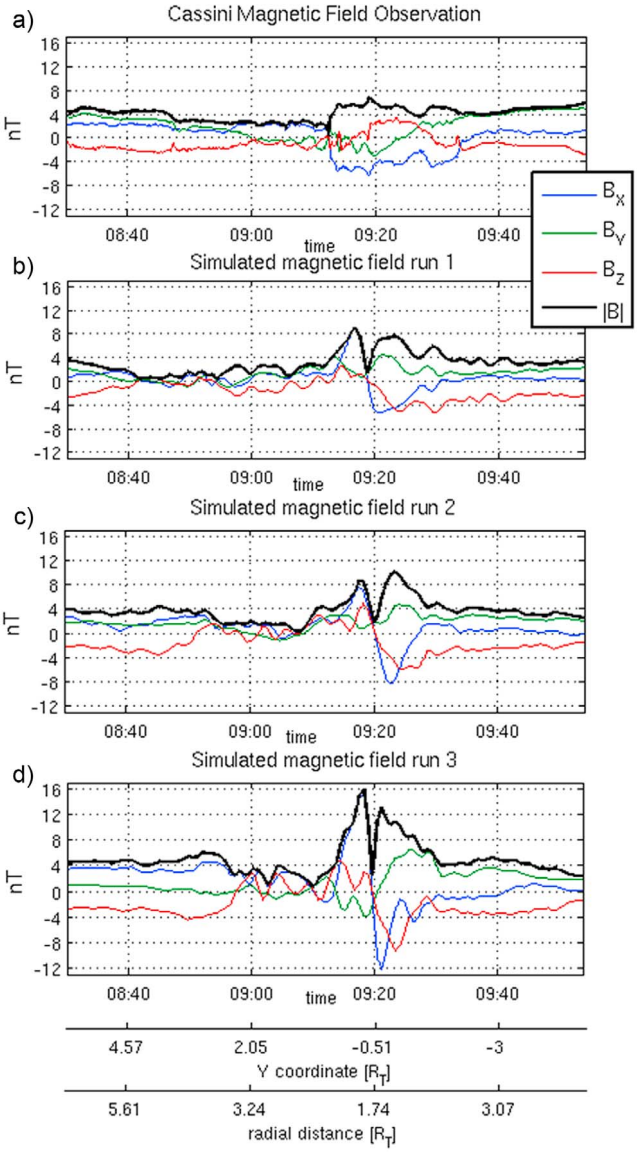

Figure 4. Magnetic field observation by the Cassini magnetometer and simulated magnetic fields along the T15 flyby trajectory for the three simulation runs. All vertical axes are from −13 to 17 nT.

lines drape around the conductive ionosphere creating two oppositely polarized tail lobes; during ideal southward orientation of the upstream magnetic field the wake north of the orbital plane has magnetic fields that are against the upstream flow (in −X direction), while the southern side has a magnetic field orientation parallel to the ambient flow (+X). These magnetic tail lobes are separated by a current sheet that is in the wake and along the orbital plane (for further details see *Neubauer et al.* [1988] and *Ness et al.* [1982]).

[49] In general, however, the current sheet is orientated along a plane that is perpendicular to the direction of ambient magnetic field (or along the plane determined by the flow direction and the convection electric field $\vec{E}_C$). In the case of the T15 flyby when the magnetic field had the largest component toward Saturn (+Y), the Cassini trajectory would have entered first the lobe with the magnetic polarization parallel to the ambient flow and located more on the side of Saturn in Titan's wake. Then the spacecraft would have crossed the current sheet into the anti-Saturn sidelobe with antiparallel magnetic field.

[50] Based on the above description the abrupt change seen in the X component of the magnetic field can be taken to indicate the location of the tail current sheet. The observed location of the current sheet of Titan's induced magnetosphere makes it possible to estimate the direction of the incident plasma flow (this was used in the case of the T9 flyby to estimate the flow direction as 30° outward of the corotational direction [see *Kallio et al.*, 2007]. In all three simulations the current sheet signature is seen at the 09:20 UTC location along the Cassini trajectory, which then corresponds exactly to a 16° deflection of the flow away from Saturn. This deflection corresponds exactly to the outward flow direction of the INUM moments used for the flow in the simulations.

[51] In the magnetometer data the drop in B_X takes place earlier at 09:12 UTC ($Y_{TIIS} = +0.44\ R_T$), which corresponds to the current sheet being bent about 13° toward Saturn! This could mean that the flow during the flyby had actually a Saturnward component; indication of this can be seen in the INUM moments as the radial velocity component in Saturn-centered coordinates changed its sign immediately before the spacecraft entered Titan's interaction region (around 08:30 UTC), although the turning of the spacecraft at the time may have interfered with the CAPS measurements (see Figure 2d). However, as the flyby was in the near wake of Titan or even within its ionosphere, it is possible that this "polarity reversal" does not fully correspond to the magnetotail neutral sheet.

[52] In the magnetometer data there is only a modest increase in the positive B_X values before the current sheet crossing (08:57 to 09:10 UTC). However, the simulation results show a large increase of the X component of the magnetic field before the current sheet signature. Further, for the three runs the electric current in the current sheet in Titan's wake increases (i.e., the drop in B_X increases) with the increased oxygen content in the magnetospheric flow. The largest absolute magnetic field value of 16 nT along the flyby trajectory is found in simulation run 3 right at the current sheet signature, while for the two other runs the maxima at the polarity reversal are around 10 nT. The probable cause for the difference between these field maxima is the larger dynamic pressure of the plasma flow due to higher oxygen density exercised a larger forcing on the magnetic tail and resulted also in the magnetic interaction region being more compressed. Previous simulation studies have shown that the magnetic pileup above Titan's conductive ionosphere can become more substantive if the mass flux of the plasma flow is increased [*Sillanpää*, 2008, section 7.3]. This change in the magnetic pileup was also seen between the simulation runs made for this study with the magnetic pileup being the most substantive in simulation run 3 (not plotted).

[53] The maximum magnetic field observed by the magnetometer was only about 7 nT. There are reasons to suspect that this discrepancy in the magnetic field values of the magnetometer measurements and the simulations is tied to the difference in the angle of bending of the current sheet between the simulation runs and the magnetometer data. The simulation results indicate that the diamagnetic effect of high-density ionotail reduced the observed magnetic field up to location 09:10 UTC. In the simulations the current sheet was passed later and while the magnetic field suppression ended about in the same location for the simulations as in the magnetometer data, the magnetic lobe on the Saturn side was not suppressed in the simulations like likely happened during the T15 flyby.

[54] The magnetic field profile also demonstrates the extent of Titan's magnetic interaction region during the flyby. In the Cassini magnetometer data the drop in the absolute magnetic field from 4.5 to below 3 nT is seen at 08:46 UTC. This timing is somewhat earlier than that seen for the drop in the absolute magnetic field in runs 2 and 3 at around 08:52 and 08:55 UTC, respectively (Figures 4c and 4d). On the other hand, for run 1 the interaction region begins already after the trajectory location 08:30 UTC. The fourth simulation run (not shown), which had no oxygen ions in the upstream flow, resulted in a very extended interaction region for Titan: the absolute magnetic field dropped to 2 nT before the location 08:30 UTC along the Cassini trajectory and then further to values below 1 nT. Therefore it is seen that with higher mass density of the plasma flow and therefore increased flow pressure, the magnetic interaction region is confined to a smaller area.

6.2. Plasma Density From Langmuir Probe

[55] In hybrid simulations the electron density is equal to the total ion density, as per the assumption of quasi-neutrality (equation (2a)). The Langmuir probe (LP) included in the Cassini Radio and Plasma Wave Science investigation provides accurate density and temperature measurements of the local electron population. Here we use the LP electron density measurements to compare with the simulation results (electron temperature is not propagated in the HYB model and cannot be obtained directly).

[56] The Langmuir probe consists of a 5 cm spherical sensor made of titanium and coated with TiN. The sensor is mounted on a 1.5 m tripod boom [*Gurnett et al.*, 2004]. The probe samples the current from the surrounding plasma while the bias voltage is varied on the sensor (in the range ±32 V during the T15 flyby). This method foremost yields values for the plasma density and electron temperature, but other space plasma parameters may be inferred as well.

[57] The instrument can measure accurately cold and dense ($n_e > 5\ \mathrm{cm}^{-3}$) plasmas, as its usefulness is limited by the Debye shielding length. However, this does not pose a serious limitation when the spacecraft is within Titan's interaction region. (Furthermore, a proxy method can be employed for

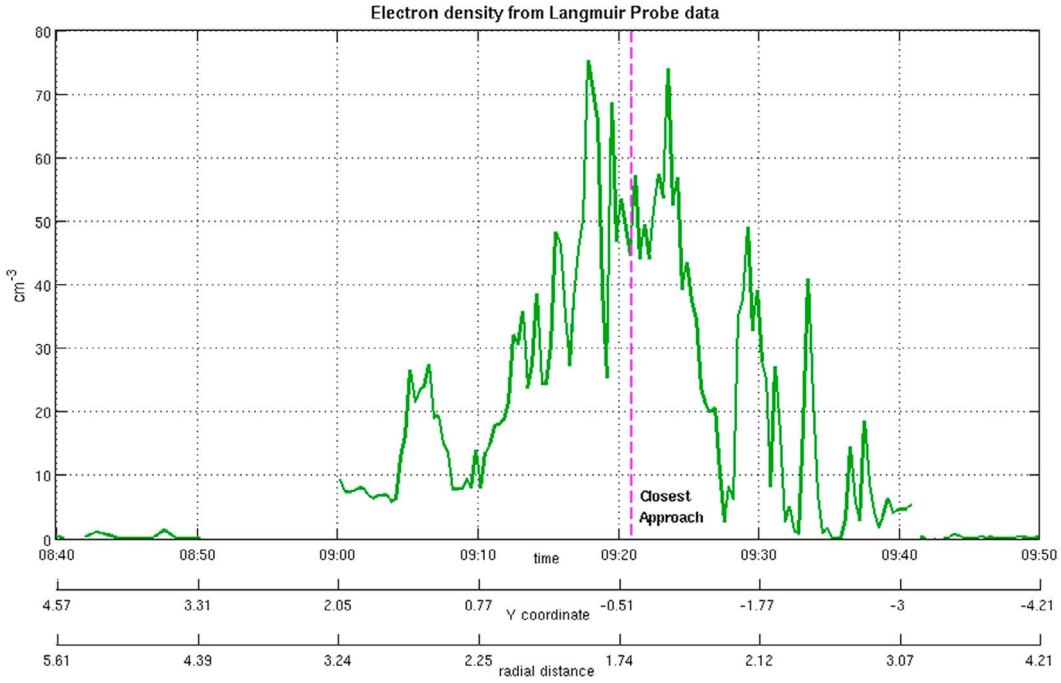

Figure 5. Langmuir probe electron density during the T15 flyby. There are some gaps in the data, i.e., from 08:50 to 09:00 UTC.

reliable estimates of lower plasma densities [*Morooka et al.*, 2009].)

[58] The LP electron density n_e is shown in Figure 5. The electron density peaks twice above 70 cm^{-3} about 3 min before and after the closest approach, while at the closest approach the density is 50 cm^{-3}. The ingress shows a rather smooth development with the main rise in the density from 10 cm^{-3} at 09:10 UTC to the maximum at 09:18 UTC. There is, nevertheless, a prominent peak exceeding 25 cm^{-3} around 09:07 UTC before the incline. In the egress of the flyby the density is fluctuating strongly between 10 and 40 cm^{-3} until settling below 10 cm^{-3} around 09:39 UTC after which point the density values here are no longer accurate.

[59] The densities of the ion species along the flyby trajectory together with the total ion density (that corresponds to electron density, n_e) for the three simulation runs are shown in Figure 6. The differences in upstream flow composition between the runs is seen in the level of the O^+ density (red line). There are several features in the simulation results for ion densities that call for attention: 1) The area where pickup ions dominate the ion density is smaller when the dynamic pressure of the flow is higher. For run 2 this area is from 08:50 to 09:40 UTC. The change in the size of this area is likely caused by the higher flow pressure being balanced closer to Titan's ionosphere. This also corresponds well with the magnetic interaction areas seen in the simulation results in section 6.1. 2) The dominant ion species in Titan's wake is molecular nitrogen. This is discussed in section 7.1. 3) The density of atomic hydrogen decreases in Titan's wake by a factor up to 5 from the upstream value of 0.07 cm^{-3}. There is also a less pronounced decrease in the water group density in the wake that coincides with the pickup ion dominated region. Similar results have been reported from our Titan simulations previously [*Sillanpää et al.*, 2007]. 4) The densities of methane and molecular hydrogen ions drop in the shadow of Titan (09:19–09:32 UTC). This is due to the production functions for these ions being based only on photoionization.

[60] In run 1 the pickup ions dominate the ion density already at the flyby location 08:40 UTC (Y = 4.5 R_T), while the increase of the pickup ions in runs 2 and 3 is sharp around 08:50 and 08:55 UTC, respectively. At these locations the total ion density increases about tenfold. On the other hand, the decrease of pickup ions in the egress part of the trajectory is more abrupt for runs 1 and 2 (around 09:35 UTC) than for run 3, in which the ambient ion density is reach at 09:45 UTC.

[61] Titan's ionotail, which is formed of cold, slow moving ions, differs in shape in the simulation runs (plots not shown). The differences in the shape and extent of the ionotail between the simulation runs are what causes the differences particularly in the falloff of the densities of the exospheric ions at the edges of the wake region as seen in Figure 6.

[62] The pickup ion trajectories are controlled by the convection electric field, which in this case points southward and away from Saturn (we ignore here the effect that the relatively small X component of $\vec{E}_C$ might have). Ions are efficiently being picked up into the passing plasma flow in regions where the electric field points away from Titan, being controlled there mostly by the $\vec{E} \times \vec{B}$ drift. In addition, there is a plasma region of very slow moving exospheric ions that extends from the wakeside ionosphere. This ionotail is especially strong when the Sun is on the ramside or on the Saturn side of Titan (Saturn local time is 18 h or 24 h, respectively; SLT was 21.20 h during the T15 flyby) when ions on the sunlit side of Titan with high ion density cannot be efficiently picked up by the plasma flow. In the HYB model we also see a strong bending of the ionotail thus formed in the opposite direction of the convection electric field (see

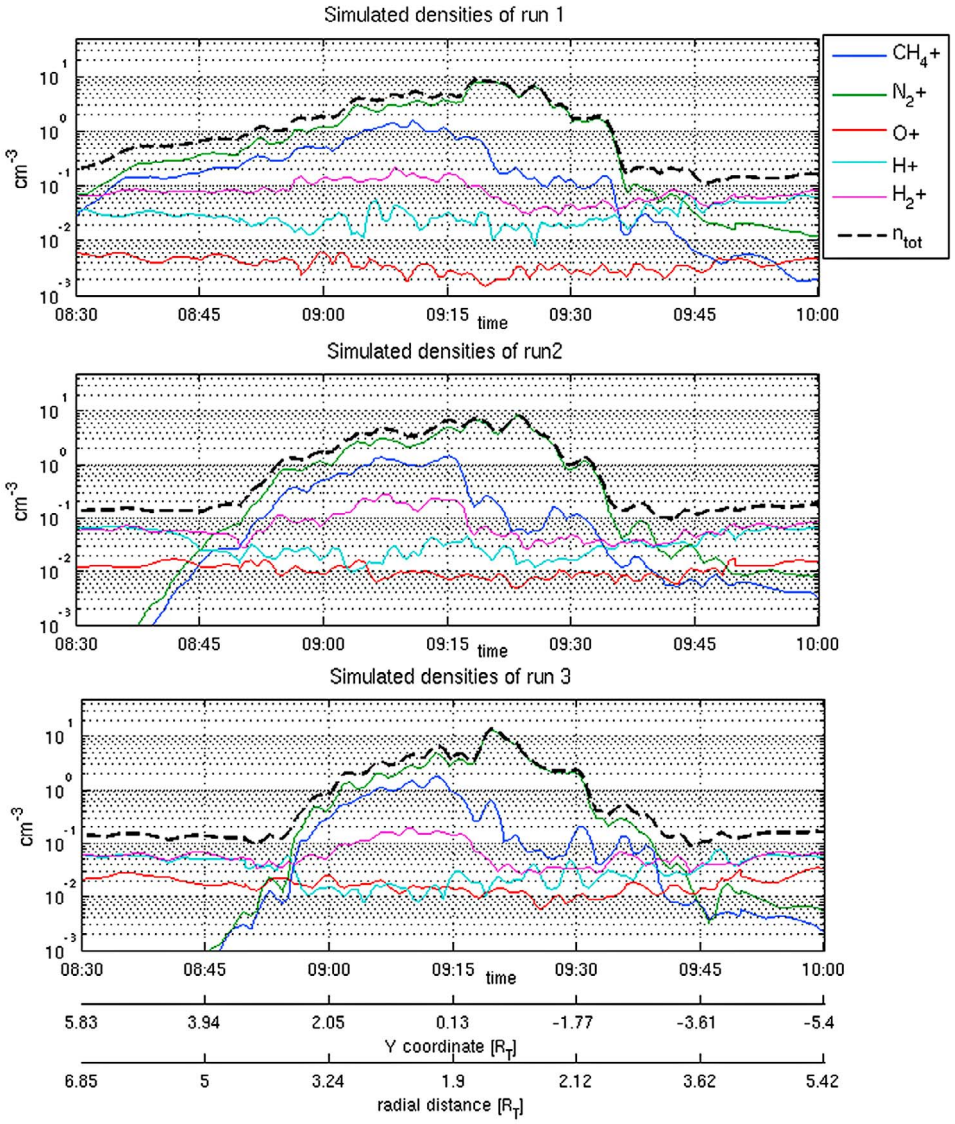

Figure 6. Simulated ion densities along the T15 flyby trajectory for the three simulation runs. The range for the vertical axes is 0.001 to 50 cm^{-3}.

Sillanpää et al. [2006]; for a physical explanation, see *Sillanpää* [2008, section 3.3.1]).

[63] In run 3, where the oxygen density in the upstream flow is the highest, the ionotail is very wide close to Titan, covering much of the northern and wakeside ionosphere and extending downstream and northward up to 2 R_T. On the equatorial plane the ionotail extends several Titan radii into the wake and is bent slightly toward Saturn and narrowing quickly in width. The ionotail boundary on the Saturn side is fairly sharp in contrast to the fluctuating anti-Saturn side boundary that is hard to locate precisely. This is consistent with the difference seen in the interaction region edges in the LP electron density.

[64] In runs 1 and 2 the ionotail extends less northward and is there wider than in run 3. The bent of the ionotail toward Saturn in the equatorial plane is also more pronounced. The Saturnward tilt is the largest in run 1 with about 45° starting from the ramside, where the ionosphere is much thicker than in the other two runs. This causes the ionotail to cover much of the ingress trajectory of the flyby in run 1, leading to the rather smooth increase in ion density. The boundary of the ionotail on the egress side for both runs 1 and 2 is sharp on the equatorial plane. In the case of the no-oxygen run 4, the ionotail is mostly indistinguishable from the extended ion cloud around Titan.

[65] It is worth noting that the direction of the convection electric field (that is determined by the direction of the ambient magnetic field) dictates the orientation of the ionotail and much of the structure of Titan's wake, like the current sheet. In the case of the T15 flyby both the magnetic lobes were crossed by the flyby trajectory, while the main ionotail was north of the trajectory as per the simulations.

[66] It is usually possible to determine the INUM moments whenever sufficient number of ions are detected within the field of view of CAPS/IMS instrument. These moments are available for the pass of Titan's wake during the T15 flyby. We use the sum of INUM density moments for the three ion groups during this flyby (see Figure 2) to test the feasibility of

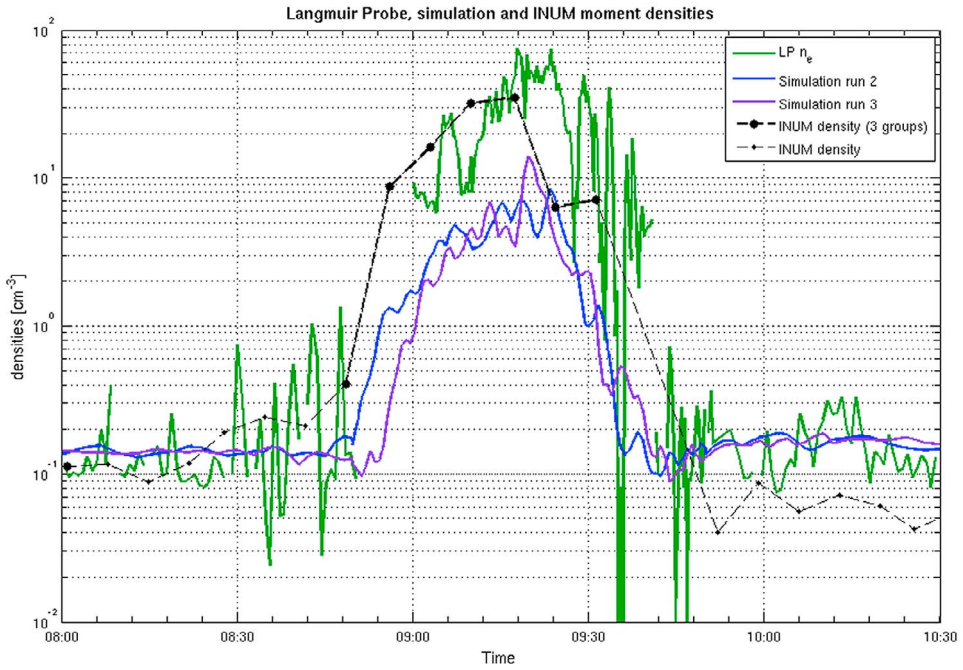

Figure 7. Comparison of LP n_e, the total ion densities from two simulation runs and the INUM density moments summed. A thicker line is used for the INUM density when values for all three ions groups were available.

using INUM moments near Titan where ion composition is more complex than in the magnetospheric plasma flow (INUM moments do not account, e.g., for N^+ and N_2^+ ions that are important at Titan). The CAPS/IMS field of view included the nominal corotation direction until 09:50 UTC and also the spacecraft ram direction around the closest approach.

[67] The LP n_e, INUM moment density sum, and total ion densities for simulations run 2 and 3 along the flyby trajectory are plotted together in Figure 7. Comparing the LP density to the simulation results shows that the simulated ion densities (that correspond to electron density) are lower by an order of magnitude than the peak densities of the LP measurements, with only run 3 reaching 10 cm^{-3}. Possible reasons for this discrepancy are considered in section 7.1. Nevertheless, the region dominated with the pickup ions in runs 2 and 3, seems to correspond well to the area where elevated n_e was detected (09:00–09:35 UTC). Unfortunately the ingress shoulder is omitted in the LP data by a measurement gap from 08:50 to 09:00 UTC. This might have helped determine whether run 2 or 3 represented the location of the edge of the interaction area better in the ingress. Overall, the ion density in run 2 seems to represent the general shape of the LP data even if the absolute density values are much smaller; the areas of highest plasma density coincide around the closest approach (09:15 to 09:24 UTC). Even the lesser peak in the LP data at 09:07 UTC reaching 25 cm^{-3} seems to have a counterpart in the run 2 results at the same location even though the simulated density is no more than 5 cm^{-3}.

[68] There is an obvious time shift between the LP electron density and the total of the INUM density moments; that seems solely caused by the INUM moments being assigned to the time at the beginning of the accumulation period of the ion counts. With the shift accounted for, the total INUM densities provides a reasonable fit to the LP electron density, especially in the shape of the signature. The maximum of the sum of the INUM densities is 35 cm^{-3}, while the LP n_e reaches momentarily over 70 cm^{-3}. This difference is likely in part due to the low time resolution of the INUM moments that is several minutes; taking an average of the LP data over the INUM moment calculation interval gives a difference between the maximum densities that is around 15 cm^{-3}. Also notable is that the INUM moments do not account for ion species outside the mass ranges used for the three groups (atomic and molecular hydrogen and water group ions), while several other ion species (e.g., atomic and molecular nitrogen ions with masses 14 and 28 amu) exist in Titan's exosphere and ionosphere. Furthermore, while water group ions overlap the methane mass (16 amu), their signature differ on the IMS straight-through analyzer, because of the additional O -signature created by ions with oxygen atoms.

6.3. CAPS Ion Observations

[69] Figure 8a shows CAPS energy spectrogram from the IMS electrostatic analyzer, while Figures 8b–8c are plotted average energies of the ion species along the flyby trajectory from the three simulation runs (Figures 8a–8d are vertically aligned to make comparisons easier). The vertical striping in the IMS spectrogram is caused by actuation of the CAPS instrument. Two energy peaks can be seen in the energy spectrogram during the ingress from 08:00 to 08:50 UTC (indicated with red and yellow lines); there is a significant drop in the energies of both peaks at 08:25 UTC. IMS time-of-flight data summed over the 30 min period starting at 08:25 UTC (not shown) indicates that there are three ion populations present: H^+, with an energy peak around 60 eV,

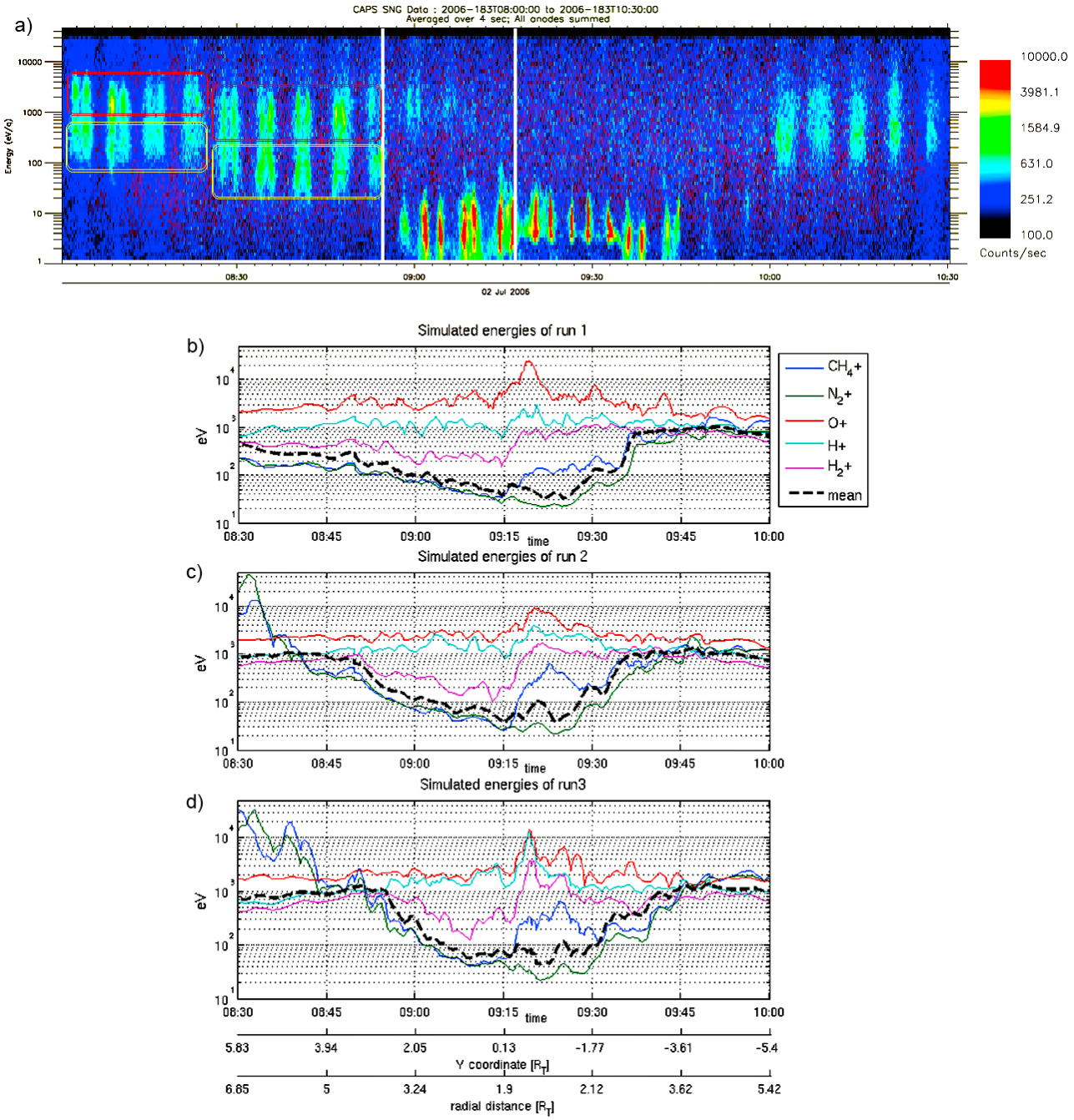

Figure 8. (a) The CAPS ion energy spectrogram of the T15 flyby and (b-d) the mean ion energies along the flyby trajectory from three simulation runs. The effect of the spacecraft velocity was taken into account in the simulation energies. CAPS/IMS ion count rate is a function of energy and time during the T15 flyby. The tick interval on the horizontal axis of Figure 8a is 3 min.

and extending from 15 to 600 eV; H_2^+, with energies peaking around 150 eV, and extending from 30 to at least 500 eV; and water group ions at 500–2000 eV.

[70] After the short data gap at 08:55 UTC the main wake region is entered with the main energy peak at 1–10 eV. In the time-of-flight data there are signatures for H^+, H_2^+, N^+, and ion species with mass 16 amu (without oxygen signature, likely CH_4^+) and 28 amu. The high-energy signature at 1000 eV continues some 10 min into the wake region consisting of both H^+ and water group ions. However, at 09:12 UTC, the high-energy counts can no longer be discerned, while the total count rate at the same time almost triples.

[71] After the second gap at 09:17 UTC the low energy peaks climb to an energy range 6–15 eV. The same constitutes exist as in the previous interval, with reduced relative abundance of the lighter ions (H^+ and H_2^+). The increase in energy takes place because of the negative charging of the spacecraft in Titan's shadow. The effect is seen in an area

that is slightly broader than the shadow of Titan's solid body (09:19–09:32 UTC). During the flyby the count rate of the CAPS electrostatic analyzer first increases by about sixfold (at 09:00 UTC) and further triples (at 09:12). The count rate steadily decreases between 09:30 and 09:50 UTC until leveling at the rates seen before Titan's interaction region.

[72] The return of the high energy ambient plasma is seen after a period of very low counts at 09:45–10:00 UTC. After 10:00 UTC the time-of-flight data (with the a poor viewing) shows a very weak (if any) signature for water group ions, while hydrogen signatures (both H^+ and H_2^+) are fairly strong.

[73] Interestingly, the region in the ingress, when the region of Titan's magnetic interaction region was entered (the magnetic field magnitude in the magnetometer data dropped below 3 nT) as presented in section 6.1, does not coincide with the onset of the cold plasma region seen in the CAPS ion data (compare Figure 3). In the simulations these regions coincide almost perfectly.

[74] The simulation results offer additional insight into the observations of the ion energies. The average energies of the different ion species in the three runs are plotted as found along the Cassini trajectory in Figures 8b–8c. The energy corresponding to spacecraft velocity was added to each ion species before plotting (about 3.5 eV for CH_4^+ and 6 eV for N_2^+). Also the mean energies for ions in the simulations are calculated and presented; however, the spread of the ion energies for any ion species in the simulation was not analyzed. The two peaks seen during the ingress in the energy spectrogram are well in line with the H^+ and O^+ mean energies as expected (INUM moment calculations are based on IMS data and the INUM moments were used for the upstream conditions in these simulations). The simulated H_2^+ mean energy, however, consists of both flow ions and exospheric ions that are mass loading the flow, which explains the lower average energy than expected from the INUM moments for these ions.

[75] The main feature in the simulation results is the drop in the average ion energy in the ionotails seen in Figure 6 (the mean ion energies are anticorrelated with the total ion densities). In runs 2 and 3 the areas with low mean ion energies coincide with the area of cold ionospheric plasma in the CAPS energy spectrogram (about 08:55–09:45 UTC) whereas in run 1 the signature for the ionotail begins already around 08:50 UTC if not at an even earlier location. The obvious difference between the IMS energy plot and the simulations is that the average simulated energies of the pickup ions remain above 20 eV along the flyby trajectory. This is likely connected to the reasons why the higher plasma densities detected by LP probe where also not seen in the simulation runs (discussed in section 7.1).

[76] The main difference between the results of the runs themselves is the extent of the main interaction region along the flyby trajectory, similarly to the simulated ion densities (see section 6.2). This region is marked by the average ion energy in the simulations dropping at least by a factor of 2 from the upstream values; here we use a limit of 300 eV for the mean ion energy (the varied oxygen density between the simulation runs did not considerably change the average ion energy in the upstream). In the ingress this energy level is reached at location 08:35 UTC in the case of run 1, at 08:52 in run 2, and in run 3 at about 09:00. In run 1 the decrease in mean ion energy is very gradual in contrast to the other two runs, where it is much more abrupt.

[77] The ions originating from Titan and its exosphere have low energies in areas where they are numerous, because the diamagnetic effect of the areas with high plasma density is shielding the ions from the energizing electromagnetic fields. Where the flyby trajectory is in Titan's shadow, methane and molecular hydrogen ions were not created locally in the simulation. That means that the ions of these species that are seen there, have migrated there and are therefore somewhat energized in contrast to N_2^+ that is created uniformly from the ionosphere in the simulations. Furthermore, the densities of these ion species created by photoionization process fall by a factor of 4 for molecular hydrogen and at least by a factor of 10 for methane when Titan's shadow is entered (see Figure 6). The few pickup ions that are seen outside the pickup-ion-dominated area (around 08:30 UTC in runs 2 and 3), have experienced a period of rapid acceleration in order to move far to one side of Titan, thus having energies exceeding 10 keV (their densities are, however, completely insignificant).

[78] The energies of the upstream species H^+ and O^+ remain somewhat level throughout the interaction region, but they do offer some insight into how much these ions are able to penetrate into Titan's wake, also relevant to what was discussed in connection with Figure 6. For H^+ the energies are the highest in run 3, even reaching the mean energies of O^+, that were also elevated. The elevated energies of the incident ions in Titan's wake are not likely due to any energization process at Titan, but rather by deflection of less energetic ions (i.e., low magnetic rigidity) that are not able to enter Titan's wake. Therefore for hydrogen ions very high energies are needed to penetrate the condense wake region of run 3. The density drop of hydrogen ions in Titan's wake was also the largest among the simulation runs. In contrast, for oxygen ions the average energies in the wake along the trajectory are highest in run 1. This could mean that the expanded interaction region in run 1 is a more difficult obstacle for oxygen ions to enter than the spatially smaller main interaction regions in runs 2 and 3, even with their more substantial magnetic pileup regions. The large gyroradius of oxygen ions may explain this effect: it is 4000 km (1.6 R_T) for the bulk velocity in the upstream. Therefore to divert oxygen ions from their original path it takes a longer period of time and a longer path in the disturbance caused by Titan's plasma interaction than for lighter hydrogen ions with a much smaller gyroradius and magnetic rigidity.

[79] As mentioned above, the incident ion signature vanishes in the wake in the CAPS observations. However, the simulations show a strong presence of the upstream ions also there. According to the simulation results the streamlines of the bulk motion of O^+ ions were deflected by 10° to 15° in the anti-Saturn direction in Titan's wake at the distance of the closest approach in run 2 (not shown). The deflection was between 15° and 20° in run 3, while in run 1 there was no deflection. The deflection angle increased toward the anti-Saturn side of the wake in runs 2 and 3. In run 2 there was also a strong northward component for these streamlines. No clear pattern was seen for streamlines of the hydrogen ions (these had larger thermal velocities and statistics may have not been sufficient). While the nominal corotation flow direction was in the field of view of the IMS instrument, as was also the INUM estimate of the upstream

flow direction (though closer to the edge of the field of view), the additional deflection found in the simulation runs 2 and 3 would have caused the main portion of the oxygen ions to be out of the IMS field of view and thus be undetectable. As for the hydrogen ions, it is possible that they too experience a deflection in Titan's wake, even if the simulations could not verify their flow direction there. Further, their simulated densities fell more drastically in Titan's wake than that of oxygen ions. That may have been enough to explain their nondetectability above the background in the IMS energy spectrogram. The sudden disappearance of the lower magnetospheric energy peak at 08:55 UTC seems to point toward that possibility (the drop in atomic hydrogen density in run 3 happens at the same location).

7. Discussion

[80] Titan's interaction with the surrounding plasma flow is subject to changes on multiple timescales; particularly the plasma density can vary by orders of magnitude. This makes it important to investigate the response of the interaction to different ambient conditions that are likely to occur. One such set of conditions is a low-density plasma flow, often referred to as "lobe-like" flow which points to the often found conditions in Saturn's magnetospheric lobes in contrast to the flow in the plasma sheet environment. The differences between these two magnetospheric flow types, that Titan encounters, are not only the absolute plasma density of the flow but also in the composition: the water group ions often dominate or provide a large fraction of the flow ions in the plasma sheet, while in the lobe-like flow water group ions are nearly nonexistent and the flow consists almost solely of hydrogen ions (both atomic and molecular).

[81] In this work we have studied the effects of small variance of the water group ion content, more exactly the O^+ density, in the plasma interaction of Titan using the global hybrid model HYB. The studied case was Titan flyby T15, where the results of multiple instruments were available to provide a "reality check" through analysis and comparisons with the model results. The model included three separate ion species for the flow, each with their own thermal velocity. As such, it cannot be always determined, based on these simulations alone, whether the differences between the simulation runs should be attributed to the change in incident ion composition, change in the upstream plasma density, or the dynamic pressure of the flow. In the analysis in section 6 we have often assumed that the change in dynamic pressure caused the seen changes in the size of Titan's plasma interaction region. Overall, the simulation results showed that changing only the density of oxygen ions in the upstream between 3 and 12 per cent of the light ion density (that was constant) is enough to change Titan's plasma interaction and especially cause significant changes in the width of the interaction region and in the bending of Titan's ionotail.

[82] In general the hybrid model results compared well with the observations by the instruments of the Cassini spacecraft and allowed several additional insights via comparisons between the simulation runs. We also feel that based on the comparisons it is possible assess that the oxygen density of the upstream plasma flow was near the run 2 value 0.008 cm^{-3} during the T15 flyby.

[83] Run 1 showed a clearly expanded interaction region especially toward Saturn, that did not correspond to Cassini observations. This expansion was in part due to the ingress of the flyby trajectory coinciding with the bent ionotail in run 1. Runs 2 and 3 showed compressed interaction regions with more abrupt edges on the ingress side both in magnetic field and in ion properties. Run 3 with higher oxygen density in the upstream flow had the smaller interaction area of these two runs. The LP n_e density had a data gap during the ingress when the cold plasma region was entered so it could not provide a check for the interaction region width in the ingress. However, the shape of the LP density profile fit better with run 2. Also run 2 corresponded better to the magnetometer observations, particularly to the start of the reduced magnetic field magnitude and by having lower and more comparable magnetic field magnitude around the closest approach. Nevertheless, there were a few features in the comparisons between the simulation runs and Cassini measurements that called for some additional discussion.

7.1. Further Comments on Comparisons

[84] There was a large disparity between the observed electron densities in the Titan's wake by the Langmuir probe and the total ion density in the simulation runs. The shape the high-density region in the wake was similar in the LP measurements and run 2, but the simulated ion densities remained mostly below 10 cm^{-3}, whereas the LP electron density reached at times 70 cm^{-3} (see Figure 7).

[85] A plausible explanation can be arrived at by examining the additional difference between the simulated and detected ion energies in the main wake region (see Figure 8). The pickup ion energies in the simulations never fall below 20 eV. The IMS energy spectrogram shows energies peaking from 3 to 10 eV. This seems to indicate that the simulation runs do not produce or contain enough of the slow moving, low-energy part of the pickup ion population in the ionotail. There are a few things to consider here. No exospheric population of atomic hydrogen was included in the simulation model; that could have a significant contribution to the total ion density in Titan's exosphere [e.g., *Garnier et al.*, 2007]. Furthermore, the simulated methane abundance seems too small in comparison to the N_2^+ abundance in the wake based on time-of-flight data. This will very likely be rectified by inclusion of more realistic production of molecular nitrogen ions (e.g., taking into account the day-night side effects). However, the time-of-flight data does not have sufficient time resolution to determine whether the shadowed portion of the cold ion region had different composition from the part that was sunlit; this could have helped identify the creation mechanisms for the ions in the cold plasma region.

[86] The model numerics is also likely to play a role: only a limited number of simulation particles (though a large number) are used to represent the ions. Regions with large density gradients like the edge of the ionosphere can be especially problematic in this regard. Further, the ions with the lowest energy can be the most difficult to model in a dynamic environment where the model numerics can cause much more acceleration for low-energy particles than exists in reality. Thus it seems that there are several possible reasons why the model did not create or contain a sufficient

number of ions to correspond to the densities measured by the LP probe.

[87] The other significant difference between simulations and the observations by the Cassini instrumentation, namely, the difference in the locations of the current sheet signature, is briefly discussed in section 6.1. Even though we sought to determine the direction of the ambient plasma flow precisely using the INUM moments, it seems that there were changes in the flow direction close to the time of the flyby as seen in the sudden change of v_r moments at 08:20 UTC (see Figure 2d). Moreover, the ambient flow direction could not be reliably determined after the closest approach. Possible changes in the flow direction during or close to the time of the flyby would have affected especially the successfulness of the comparison of the magnetometer observations to the magnetic fields of the simulation runs. The ionotail, based on earlier simulation results from the HYB-Titan model, forms slowly and reacts to changes in the flow conditions with a significant delay.

[88] If we assume that the upstream was turned Saturnward about 13° rather than away from Saturn by 16° as was estimated from the INUM moments, how would this have changed the interaction? Assuming otherwise similar the flow conditions, the wake could form about the same only rotated about 30° counterclockwise around Titan's rotation axis. As we did not simulate such a case, our considerations may be partially misled by assuming that Titan's plasma environment could react in such a simplistic way. The current sheet signature in the simulations corresponded exactly to the flow direction in the simulations runs made, so like it would coincide with the signature seen in the magnetometer data. The change in the ionotail orientation is easy to estimate; such a rotation turns the ionotail in run 1 to the front side of ingress of the Cassini trajectory while in the cases of runs 2 and 3 the ionotails would be along the ingress of the trajectory. This would make the interaction regions in runs 2 and 3 to extend much further in the ingress similar to results in run 1 and in noncompliance with the plasma density and ion measurements by Cassini. While the turned run 1 would have narrower interaction region along the trajectory, it would be from the "backside" of the ionotail that is less well defined. Consequently this would not likely correspond well to the clearly defined entry into the cold plasma region seen in the LP electron density and the CAPS ion measurements. All in all, the flow direction may have shifted during the flyby but the orientation of the ionotail in the simulated case of run 2 seems to correspond best among the simulated and "turned" cases to the observations.

[89] As with any simulation model, also the HYB-Titan model used in this study, has caveats that should be pointed out. Hybrid method provides the needed ion dynamics on time and spatial scales pertinent to Titan's plasma environment, that is not always the case with other simulation approaches. While we feel confident in the noninference of outbound conditions used in the simulation and further, that the number of simulation particles used and the run time where sufficient to the purposes of this study, the main questions about the full applicability of the simulation results probably lie in particle interactions and inner boundary conditions.

[90] The fact that the ionization of the near Titan region is only provided by photoionization process and insertion of ion particles at the exobase, causes noninclusion of effects that, e.g., electron impact ionization could create (though it is of less importance than photoionization as a whole). Perhaps the most important particle interaction to implement in the future versions of the HYB-Titan model, in the charge exchange processes, that can change the incident ion fluxes in Titan's exosphere; furthermore, charge exchange can contribute to the formation of cold ion mantle around Titan [see *Szegö et al.*, 2005]. The plasma above the exobase is noncollisional, and there does not seem to be a need for inclusion of chemical reactions as the ionospheric plasma density is the effective inner boundary for the simulation model. Nevertheless, elastic collisions between exospheric neutrals and incident ions and pickup ions even above the exobase may be a significant process of deenergization for ions (and a way of heating the neutral matter), as new HYB-Titan model results indicate (paper in preparation).

[91] An interesting result was that the INUM total density compared well to the LP electron density in the cold ion region of Titan's wake. Another intriguing matter was that the edge of the IMS field of view was found as a probable cause for the nondetection of oxygen ions of the magnetospheric flow in Titan's wake due to additional analysis of the simulation data: the simulation results forrun 2 and 3 indicated that there was a further deflection of the average flow of oxygen ions away from Saturn in the wake.

7.2. Variability in Titan's Plasma Interaction

[92] The magnetospheric plasma can vary much in density and mass flux at Titan's orbit. The dynamic pressure, which is of interest here, varies by even more than two orders of magnitude between high-density cases (Voyager 1 flyby and typical plasma sheet encounters) and very low density "lobe-like" cases (e.g., flybys T9 and T18, [see *Sittler et al.*, 2010]). The T15 flyby that was studied here falls in between these two categories. Knowledge on the responsiveness of the interaction to the flow pressure would have a great significance to understanding the plasma interaction at Titan. For example, the compression of the ionosphere due to high-flux flow might not be as large as could be expected as some ionization processes would likely become more frequent, thus increasing the charge density of the ionosphere during a high density and high-pressure flow.

[93] The magnetospheric flow encompassing Titan causes a variety of physical processes to take place at Titan, that are vital in the way Titan's plasma interaction takes place. The composition, density and thermal properties of the flow all play a vital role in these processes. First, the composition contributes to the penetration depth of the flow ions into Titan's exosphere and ionosphere. Secondly, the pressure exerted on Titan by the flow affect the standoff distance of the magnetic barrier (and whether one is formed). Moreover, the thermal motion of the flow ions and the bulk flow velocity determine the gyroradius of the flow particles. As the gyroradii of the incident ions are comparable to Titan's size, the spatial distribution of the energy deposition into the ionosphere can be affected by the velocity distributions of the flow ions. Further, Titan's wake is greatly influenced as well: the flow can cause the interaction region in general to be more compressed or expanded. This can change, e.g., the bending of the ionotail. Moreover, the convection electric field that the incident flow generates at Titan, determines much of the pickup ion trajectories. In addition to the effects by the particle composition and flux and velocity of the

plasma flow, it is the ambient magnetic field carried by the flow, and especially its orientation, that determines to a large degree the orientation of the wake structures like the current sheet between the induced magnetic lobes. While many of the effects of the varying flow properties is difficult to even qualitatively predict, one that is currently even less well known is how the flow properties effect the magnetic draping around Titan's conducting ionosphere, as it is dependent on ionospheric currents and conductancies as well as on the Alfvénic Mach number, among others.

[94] The simulation results presented in this paper indicate especially the sensitivity of the extent of Titan's wake region to incident flow pressure. With increased flow pressure (via increased oxygen ion content) the wake became contracted and showed more rapid falloff at the edges of the interaction region. Comparisons with the Cassini instrument data showed how the simulations can provide insight to the ion energetics and to the composition and density features.

[95] Previous studies have often focused on Voyager 1 type or high-plasma pressure cases or in a few cases on Titan's interaction with the plasma of the magnetosheath. Our multi-instrument study of a weaker interaction case provides more breadth to the studied cases. For a comprehensive look into the Titan interaction all the various cases call for attention. As the statistics on the plasma environment of Titan continue to increase, eventually we can expect to be able to put together estimates of the occurrence of each incident plasma case.

[96] As a final note, we feel it appropriate to point out definite similarities between the plasma interactions of Titan and planets Venus and Mars. All of them are without global intrinsic magnetic field and they all have ionospheres and atmospheres that contribute to their interactions with their ambient plasma flows particularly via electric currents and particle escape. There are studies in the case of Venus and Mars of the compression of the ionosphere in cases of increased solar wind pressure [*Russell and Vaisberg*, 1983; *Russell et al.*, 2006; *Cloutier et al.*, 1999]. Such studies use events detected by long-time spacecraft orbiters for these planets. From Titan our observations are from unique (although numerous) flybys, which makes it difficult to pinpoint similar events and corresponding observations to draw direct conclusions about the behavior of Titan's ionosphere under varying plasma flow pressures. There are also two significant differences in the case of Titan. Titan has much more extended exosphere than Mars or Venus. In Titan's exosphere neutral molecules and atoms are also easily ionized, and thus it creates a diffusive region around Titan that slows down and interacts with the incident plasma flow before it reaches Titan's ionosphere. Secondly, the magnetospheric plasma flow is hot and typically subsonic in contrast to the cold, supersonic solar wind interacting with Venus and Mars. Nevertheless, the pressure balance can be assumed to play a similar role at Titan, though additional studies are needed to confirm such behavior through both observations and valid simulations.

8. Summary

[97] We have used numerical CAPS moments to quantify Titan's ambient magnetospheric plasma flow during a Cassini flyby. Several global hybrid simulation runs were made based on those values while varying the oxygen ion content of the upstream plasma flow. The simulation results for the T15 flyby were compared with the observations made by several plasma instruments onboard the Cassini spacecraft, namely the Cassini magnetometer, the Langmuir probe and the Cassini Plasma Spectrometer. These comparisons showed the effects that changes in oxygen content of the flow can have on Titan's wake region, particularly to the breadth of the cold ionotail. Key features of Titan's interaction studied include the behavior of the bent high-density ionotail and the energies of different ion species in the wake. Based on the comparisons the upstream density of oxygen ions was estimated as having been about 0.008 cm^{-3}.

[98] Comparing global simulation results with several instruments simultaneously, as was done here, is an optimal approach in order to form a comprehensive picture of the plasma interaction taking place at Titan.

[99] **Acknowledgments.** We recognize Dot Delapp from Los Alamos National Laboratory for her work that was vital to this study in providing the CAPS/IMS moments. Work on CAPS analysis was supported by SwRI contract 1356497 with JPL/NASA.

[100] Masaki Fujimoto thanks the reviewers for their assistance in evaluating this paper.

References

Ågren, K., J.-E. Wahlund, P. Garnier, R. Modolo, J. Cui, M. Galand, and I. Müller-Wodard (2009), On the ionospheric structure of Titan, *Planet. Space Sci.*, *57*, 1821–1827, doi:10.1016/j.pss.2009.04.012.

Arridge, C. S., N. André, N. Achilleos, K. K. Khurana, C. L. Bertucci, L. K. Gilbert, G. R. Lewis, A. J. Coates, and M. K. Dougherty (2008), Thermal electron periodicities at 20 R_S in Saturn's magnetosphere, *Geophys. Res. Lett.*, *35*, L15107, doi:10.1029/2008GL034132.

Bertucci, C., et al. (2008), The magnetic memory of Titan's ionized atmosphere, *Science*, *321*, 1475–1478, doi:10.1126/science.1159780.

Bertucci, C., B. Sinclair, N. Achilleos, P. Hunt, M. K. Dougherty, and C. S. Arridge (2009), The variability of Titan's magnetic environment, *Planet. Space Sci.*, *57*, 1813–1829, doi:10.1016/j.pss.2009.02.009.

Cloutier, P. A., et al. (1999), Venus-like interaction of the solar wind with Mars, *Geophys. Res. Lett.*, *26*(17), 2685–2688, doi:10.1029/1999GL900591.

Edberg, N. J. T., J.-E. Wahlund, K. Ågren, M. W. Morooka, R. Modolo, C. Bertucci, and M. K. Dougherty (2010), Electron density and temperature measurements in the cold plasma environment of Titan: Implications for atmospheric escape, *Geophys. Res. Lett.*, *37*, L20105, doi:10.1029/2010GL044544.

Garnier, P., I. Dandouras, D. Toublanc, P. C. Brandt, E. C. Roelof, D. G. Mitchell, S. M. Krimigis, N. Krupp, D. C. Hamilton, and H. Waite (2007), The exosphere of Titan and its interaction with the kronian magnetosphere: MIMI observations and modeling, *Planet. Space Sci.*, *55*, 165–173, doi:10.1016/j.pss.2006.07.006.

Gurnett, D. A., et al. (2004), The Cassini radio and plasma wave investigation, *Space Sci. Rev.*, *114*, 395–463.

Hartle, R. E., et al. (2006), Initial interpretation of Titan plasma interaction as observed by the Cassini plasma spectrometer: Comparisons with Voyager 1, *Planet. Space Sci.*, *54*, 1211–1224, doi:10.1016/j.pss.2006.05.029.

Kabin, K., T. I. Gombosi, D. L. DeZeeuw, K. G. Powell, and P. L. Israelevich (1999), Interaction of the Saturnian magnetosphere with Titan: Results of a three-dimensional MHD simulation, *J. Geophys. Res.*, *104*(A2), 2451–2458, doi:10.1029/1998JA900080.

Kallio, E., I. Sillanpää, and P. Janhunen (2004), Titan in subsonic and supersonic flow, *Geophys. Res. Lett.*, *31*, L15703, doi:10.1029/2004GL020344.

Kallio, E., I. Sillanpää, R. Jarvinen, P. Janhunen, M. K. Dougherty, C. Bertucci, and F. Neubauer (2007), Morphology of the magnetic field near Titan: Hybrid model study of the Cassini T9 flyby, *Geophys. Res. Lett.*, *34*, L24S09, doi:10.1029/2007GL030827.

Kopp, A., and W.-H. Ip (2001), Asymmetric mass loading effect at Titan's ionosphere, *J. Geophys. Res.*, *106*(A5), 8323–8332, doi:10.1029/2000JA900140.

Ledvina, S. A., T. E. Cravens, and K. Kecskeméty (2005), Ion distribution in Saturn's magnetosphere near Titan, *J. Geophys. Res.*, *110*, A06211, doi:10.1029/2004JA010771.

Ma, Y., A. F. Nagy, T. E. Cravens, I. V. Sokolov, K. C. Hansen, J.-E. Wahlund, F. J. Crary, A. J. Coates, and M. K. Dougherty (2006), Comparisons between MHD model calculations and observations of Cassini flybys of Titan, *J. Geophys. Res.*, *111*, A05207, doi:10.1029/2005JA011481.

Magee, B. A., J. H. Waite, K. E. Mandt, J. Westlake, J. Bell, and D. A. Gell (2009), INMS-derived composition of Titan's upper atmosphere: Analysis methods and model comparison, *Planet. Space Sci.*, *57*, 1895–1916, doi:10.1016/j.pss.2009.06.016.

Modolo, R., G. M. Chanteur, J.-E. Wahlund, P. Canu, W. S. Kurth, D. Gurnett, A. P. Matthews, and C. Bertucci (2007), Plasma environment in the wake of Titan from hybrid simulation: A case study, *Geophys. Res. Lett.*, *34*, L24S07, doi:10.1029/2007GL030489.

Morooka, M. W., et al. (2009), The electron density of Saturn's magnetosphere, *Ann. Geophys.*, *27*, 2971–2991.

Nagy, A. F., Y. Liu, K. C. Hansen, K. Kabin, T. I. Gombosi, M. R. Combi, D. L. DeZeeuw, K. G. Powell, and A. J. Kliore (2001), The interaction between the magnetosphere of Saturn and Titan's ionosphere, *J. Geophys. Res.*, *106*(A4), 6151–6160, doi:10.1029/2000JA000183.

Ness, N. F., M. H. Acuña, and K. W. Behannon (1982), The induced magnetosphere of Titan, *J. Geophys. Res.*, *87*(11), 1369–1381.

Neubauer, F. M., D. A. Gurnett, J. D. Scudder, and R. E. Hartle (1988), Titan's magnetospheric interaction, in *Saturn*, edited by T. Gehrels and M. Shapley Matthews, pp. 760–787, Univ. of Ariz. Press, Tucson.

Neubauer, F. M., et al. (2006), Titan's near magnetotail from magnetic field and electron plasma observations and modeling: Cassini flybys TA, TB, and T3, *J. Geophys. Res.*, *111*, A10220, doi:10.1029/2006JA011676.

Russell, C. T., and O. Vaisberg (1983), The interaction of the solar wind with Venus, in *Venus*, edited by D. M. Hunten et al., pp. 873–940, Univ. of Ariz. Press, Tucson.

Russell, C. T., J. G. Luhmann, and R. J. Strangeway (2006), The solar wind interaction with Venus through the eyes of Pioneer Venus Orbiter, *Planet. Space Sci.*, *54*, 1482–1495, doi:10.1016/j.pss.2006.04.025.

Rymer, A. M., H. T. Smith, A. Wellbrock, A. J. Coates, and D. T. Young (2009), Discrete classification and electron energy spectra of Titan's varied magnetospheric environment, *Geophys. Res. Lett.*, *36*, L15109, doi:10.1029/2009GL039427.

Sillanpää, I. (2008), Hybrid modelling of Titan's interaction with the magnetosphere of Saturn, Ph.D. dissertation, Finn. Meteorol. Inst., Helsinki.

Sillanpää, I., E. Kallio, P. Janhunen, W. Schmidt, K. Mursula, J. Vilppola, and P. Tanskanen (2006), Hybrid simulation study of ion escape at Titan for different orbital positions, *Adv. Space Res.*, *38*, 799–805, doi:10.1016/j.asr.2006.01.005.

Sillanpää, I., E. Kallio, R. Jarvinen, and P. Janhunen (2007), Oxygen ions at Titan's exobase in a Voyager 1-type interaction from a hybrid simulation, *J. Geophys. Res.*, *112*, A12205, doi:10.1029/2007JA012348.

Simon, S., and U. Motschmann (2009), Titan's induced magnetosphere under non-ideal upstream conditions: 3D multi-species hybrid simulations, *Planet. Space Sci.*, *57*, 2001–2015, doi:10.1016/j.pss.2009.08.010.

Simon, S., A. Bößwetter, T. Bagdonat, U. Motschmann, and K.-H. Glassmeier (2006), Plasma environment of Titan: A 3D hybrid simulation study, *Ann. Geophys.*, *24*, 1113–1135.

Simon, S., A. Wennmacher, F. M. Neubauer, C. L. Bertucci, H. Kriegel, J. Saur, C. T. Russell, and M. K. Dougherty (2010), Titan's highly dynamic magnetic environment: A systematic survey of Cassini magnetometer observations from flybys TA-T62, *Planet. Space Sci.*, *58*, 1230–1251, doi:10.1016/j.pss.2010.04.021.

Sittler, E. C., Jr., et al. (2010), Saturn's magnetospheric interaction with Titan as defined by Cassini encounters T9 and T18: New results, *Planet. Space Sci.*, *58*, 327–350, doi:10.1016/j.pss.2009.09.017.

Snowden, D., R. Winglee, C. Bertucci, and M. Dougherty (2007), Three-dimensional multifluid simulation of the plasma interaction at Titan, *J. Geophys. Res.*, *112*, A12221, doi:10.1029/2007JA012393.

Szegö, K., et al. (2005), The global plasma environment of Titan as observed by Cassini Plasma Spectrometer during the first two close encounters with Titan, *Geophys. Res. Lett.*, *32*, L20S05, doi:10.1029/2005GL022646.

Thomsen, M. F., and D. M. Delapp (2005), Numerical moments computation for CAPS/IMS, *Rep. LA-UR-05-1542*, Los Alamos Natl. Lab., Los Alamos, N. M.

Thomsen, M. F., D. B. Reisenfeld, D. M. Delapp, R. L. Tokar, D. T. Young, F. J. Crary, E. C. Sittler, M. A. McGraw, and J. D. Williams (2010), Survey of ion plasma parameters in Saturn's magnetosphere: Some salient results, *J. Geophys. Res.*, *115*, A10220, doi:10.1029/2010JA015267.

Tseng, W.-L., W.-H. Ip, and A. Kopp (2008), Exospheric heating by pickup ions at Titan, *Adv. Space Res.*, *41*(1), 54–60.

Winglee, R. M., D. Snowden, and A. Kidder (2009), Modification of Titan's ion tail and the kronian magnetosphere: Coupled magnetospheric simulations, *J. Geophys. Res.*, *114*, A05215, doi:10.1029/2008JA013343.

Young, D. T., et al. (2004), Cassini Plasma Spectrometer investigation, *Space Sci. Rev.*, *114*, 1–112, doi:10.1007/s11214-004-1406-4.

C. Bertucci, Institute for Astronomy and Space Physics, Ciudad Universitaria, Casilla de Correco 67 Sucursal 28, C1428ZAA, Buenos Aires, Argentina.

F. Crary, I. Sillanpää, and D. T. Young, Space Science and Engineering Division, Southwest Research Institute, PO Drawer 28510, San Antonio, TX 78228-0510, USA. (ilkka.sillanpaa@swri.edu)

E. Kallio, P. Janhunen, and R. Jarvinen, Finnish Meteorological Institute, PO Box 503, FI-00101 Helsinki, Finland.

D. Reisenfeld, Department of Physics and Astronomy, University of Montana, 32 Campus Dr., Missoula, MT 59812, USA.

M. Thomsen, Los Alamos National Laboratory, MS D466, Los Alamos, NM 87545, USA.

J.-E. Wahlund, Swedish Institute of Space Physics, Uppsala Division, Box 537, Uppsala SE-751 21, Sweden.